

---

# Optimization of a Magnetic Drive Blender Orthogonal Experiment Method and Experimental Verification

**Jianlong Gong**

School of Mechanical and Electrical Engineering, Guangdong Communication Polytechnic, Guangzhou, China

**Email address:**

[gongjianlong@gdcp.edu.cn](mailto:gongjianlong@gdcp.edu.cn)

**To cite this article:**

Jianlong Gong. Optimization of a Magnetic Drive Blender Orthogonal Experiment Method and Experimental Verification. *American Journal of Electromagnetics and Applications*. Vol. 10, No. 1, 2022, pp. 9-15. doi: 10.11648/j.ajea.20221001.12

**Received:** October 8, 2022; **Accepted:** November 2, 2022; **Published:** November 11, 2022

---

**Abstract:** In order to solve the problems of the traditional blenders, such as short service life, easy leakage and high noise, a magnetic driven blender with disc magnetic coupler as the core stirring component was designed. The experimental design was carried out by orthogonal test method. The three-dimensional software Solidworks was used to establish the structural model of the disk magnetic coupler with nine groups of different structural parameters. The finite element software Ansys Maxwell was used to carry out numerical simulation of nine groups of different structural models of the disk magnetic coupler. The range analysis method was used to study the main and insignificant factors that affect the performance of the disc magnetic coupler, and the optimal structure parameters of the disc magnetic coupler were obtained. The results show that the level values with the most significant among all factors were the permanent magnet thickness (A3), the number of magnetic poles (B3), and the air gap spacing (C1), respectively. The optimal geometric parameter structure of the disk magnetic coupler was A3=10mm, B3=12 pairs, and C1=3mm, respectively. The performance of the optimized disk magnetic coupler was improved by 88%. It provides a design reference for the following research on the performance optimization of disc magnetic coupler.

**Keywords:** Magnetic Drive Blender, Disk Magnetic Coupler, Orthogonal Test Analysis, Finite Element Analysis

---

## 1. Introduction

Traditional magnetic drive blender makes use of ultra-high rotating speed to make the knife rest collide violently with food, break the cell wall of food instantly when contacting food, and release nutrients inside food, which can not only ensure the delicate taste of food after wall-breaking, but also benefit the digestion and absorption of food by human body [1]. With the trend of consumption upgrading and health-preserving consumption concept, the market scale of magnetic drive blenders in China has been expanding in recent years, and the offline market of kitchen blenders is almost completely occupied by magnetic drive blenders, accounting for 94% [2]. The existing traditional magnetic drive blender uses a high-speed motor to directly drive the loading blade to beat the food, which has the disadvantages of short service life, easy leakage, high noise, and so on [1]. The disk magnetic coupler is a new type of transmission device. It can realize contactless transmission of force or moment, avoid the rigid connections between parts, and effectively improve the reliability and service life of the mechanical operation. Moreover, it can transform dynamic seals

into static seals, ensure no mutual penetration between working media, and realize zero leakage and low noise in the true sense [3-6]. Because of its good characteristics and wide application, more and more scholars have carried out theoretical research on disk magnetic coupler to achieve better transmission efficiency and accurate design [7-10]. Therefore, this paper proposes to use the magnetic drive in the traditional driving mode of the blender.

In this paper, a new type of magnetic drive blender is designed. The whipping structure of the magnetic drive blender mainly uses a disk magnetic driving mechanism, taking the disk magnetic coupler as the research goal. Firstly, the geometric model is established in Solidworks software, then import the finite element software, Ansys Maxwell, to establish the finite element model, the L9 (3<sup>3</sup>) orthogonal table is used to comprehensively consider the structural parametric design of permanent magnets in driving wheels, and driven wheels. Carry on the analysis of range to the results, the key factors and non-key factors affecting the output magnetic torque are determined. And a new optimized scheme is proposed according to the optimization results. This paper provides a certain reference for the design of the disk magnetic coupler.

## 2. The Basic Structure of Magnetic Drive Blender

The structure of the new magnetic drive blender is shown in figure 1. The magnetic drive blender is mainly composed of a driving wheel, a driven wheel, a bearing, a bearing bracket, a servo motor, an upper permanent magnet, a lower permanent magnet, an isolation cover, a loaded blade and so on. There is a certain distance air gap between the driving wheel and the driven wheel, and permanent magnets are uniformly

embedded in the circumferential directions of the driving wheel and the driven wheel. The permanent magnets on the driving wheel and the driven wheel are magnetized axially, and the N and S magnetic poles are staggered with each other. When the servo motor drives the driving wheel to rotate, within the distance that can be affected by the interactive magnetic force, the permanent magnets on the driving wheel and the driven wheel participate in meshing work, which will generate continuous magnetic torque, thus driving the driven wheel to rotate synchronously [11, 12].

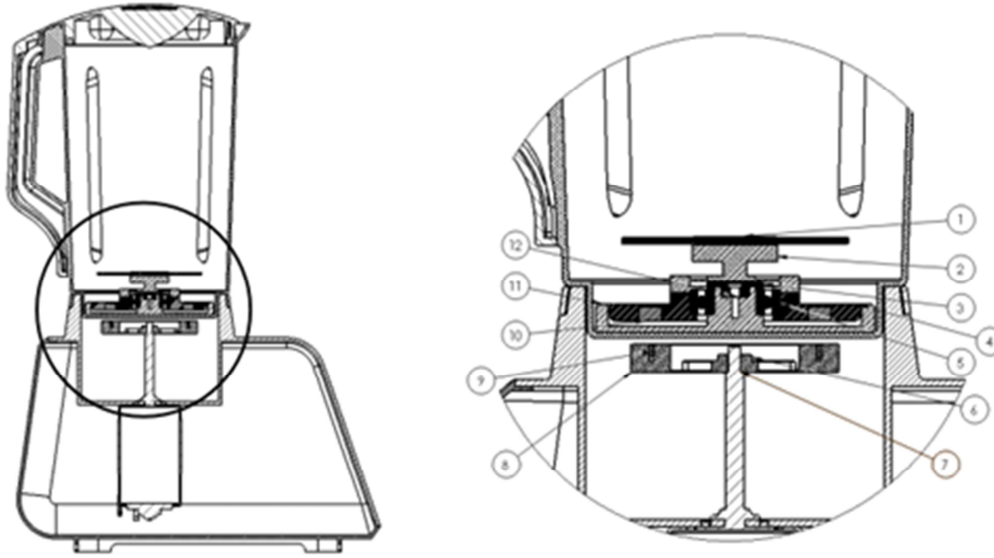


Figure 1. Magnetic drive blender section view.

1-Load blade; 2-Connector; 3-Clamping slot; 4-Base; 5-Bearing; 6-Chuck plate; 7-Drive shaft; 8-Drive wheel; 9-lower permanent magnet; 10-upper permanent magnet; 11-driven wheel; 12-Bearing bracket;

## 3. Analysis of Magnetic Characteristics of Disk Magnetic Coupler

### 3.1. Magnetic Finite Element Analysis Model

The whipping structure of the magnetic drive blender mainly uses a disk magnetic driving mechanism. In order to reduce the calculated amount of the finite element model, the disk magnetic coupler is simplified. The simplified disk magnetic coupler model is mainly composed of a driving wheel, driven wheel, permanent magnet disk, upper permanent magnet, lower permanent magnet, rotating shaft, yoke and air domain. The three-dimensional geometric model of disk magnetic coupler is established in Solidworks software, and imported into finite element software Ansys Maxwell to establish a finite element model, as shown in figure 2. In this model, the driving wheels and driven wheels are coaxially placed up and down in a disk type, the permanent magnet material is Nd-Fe-B, which needs to be set separately. The coercive force of the permanent magnet is  $-880000$  A/m. The remanence of the permanent magnet is  $1.18$  T. The relative angular velocity of the driving wheels and driven wheels is  $1500$  rad/s. The permanent magnet disk material is Steel 1010, the yoke iron material is low carbon

steel, and the region and band domains are set as the vacuum. In order to simplify the research problem and reduce the numerical calculation of the model, the following assumptions are made [12]: 1) The material in the disk magnetic coupler is isotropic, and the permanent magnet is uniformly magnetized; 2) The performance of the permanent magnet does not change with temperature; 3) The vibration and deformation of parts are not considered, and the deformation of parts during actual motion is ignored.

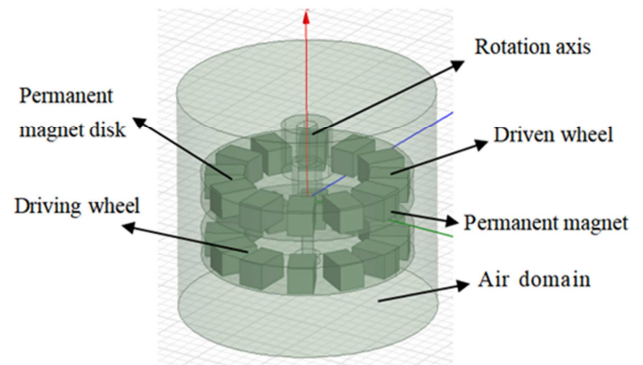


Figure 2. Finite element of disk magnetic couple.

### 3.2. Analysis of Magnetic Characteristics

The magnetic performance of the magnetic drive blender is mainly reflected in the output magnetic torque transmitted by the disk magnetic couple. So the output magnetic torque is the focus of analysis and discussion. According to the equivalent current model [13] of permanent magnets, permanent magnets can be simulated as distributions of equivalent bulk current density  $J_m$  and surface current density  $j_m$ , including:

$$\begin{cases} J_m = \nabla \times M \\ j_m = M \times n \end{cases} \quad (1)$$

In the formula (1),  $M$  is the magnetization of the permanent magnet;  $n$  is the normal unit vector of the permanent magnet surface;

The output magnetic torque of the disk magnetic coupler can be regarded as being produced by the equivalent current subjected to Lorentz force in the external magnetic field with magnetic induction intensity  $B$ . Thus, the magnetic torque of the permanent magnet in an external magnetic field  $B$  can be calculated by the formula (2).

$$T = \int_V r \times (J_m \times B) dV + \int_S r (j_m \times B) dS \quad (2)$$

In the formula (2),  $R$  is the vector diameter from the current element to the center of the disk magnetic coupler;  $V$  and  $S$  are the volume and surface area of the permanent magnet;

## 4. Orthogonal Experiment and Analysis Based on Numerical Simulation

### 4.1. Determinations of Orthogonal Experimental Factors and Levels

In this paper, the  $L_9 (3^3)$  orthogonal table is used to arrange the test reasonably [14], and the structural and working characteristics of the disk magnetic coupler are comprehensively analyzed. Three variables, including the thickness of the permanent magnet on the driving wheel and the driven wheel, the number of magnetic poles, and the air gap spacing, are selected as the orthogonal test factors, and the test level is selected as 3. In order to obtain the influence of various factors on the test index conveniently, choose the initial design size, scheme 5 in the orthogonal test as the initial basic size, and each size changes up and down based on this, and the changing range of each group is equal. Take the maximum and minimum values of factors as the changing range of factor size, and comprehensively consider the level number and size change range to select the level value of each factor. To sum up, the three-factor three-level orthogonal experimental design scheme of the disk magnetic coupler is shown in table 1.

Table 1. Three factors and three levels of radiator.

| Levels | Factors                              |                                   |                        |
|--------|--------------------------------------|-----------------------------------|------------------------|
|        | A Thickness of permanent magnet [mm] | B Number of magnetic poles [pair] | C Air gap spacing [mm] |
| 1      | 6                                    | 36                                | 3                      |
| 2      | 8                                    | 18                                | 5                      |
| 3      | 10                                   | 12                                | 7                      |

### 4.2. Orthogonal Experimental Design

An orthogonal table is a set of regular design tables. The  $L_9 (3^3)$  orthogonal table is selected according to three factors and three levels of disk magnetic coupler to arrange the experiment,

which indicates that nine experiments need to be done [14]. Finite element software was used to conduct nine experiments, respectively, which obtained the magnetic torque of the disk magnetic coupler model, as shown in table 2.

Table 2. Experimental arrangement and results.

| Test Serial number | Factors                              |                                   |                        |                       |
|--------------------|--------------------------------------|-----------------------------------|------------------------|-----------------------|
|                    | A Thickness of permanent magnet [mm] | B Number of magnetic poles [pair] | C Air gap spacing [mm] | magnetic torque [N·m] |
| 1                  | 6                                    | 36                                | 3                      | 10.6                  |
| 2                  | 6                                    | 18                                | 7                      | 1.6                   |
| 3                  | 6                                    | 12                                | 5                      | 13.8                  |
| 4                  | 8                                    | 36                                | 7                      | 1.6                   |
| 5                  | 8                                    | 18                                | 5                      | 12.5                  |
| 6                  | 8                                    | 12                                | 3                      | 22.0                  |
| 7                  | 10                                   | 36                                | 5                      | 4.1                   |
| 8                  | 10                                   | 18                                | 3                      | 21.0                  |
| 9                  | 10                                   | 12                                | 7                      | 12.0                  |

### 4.3. Analysis of Design Results of Orthogonal Experimental Table

In order to get the relationship between the goal and each

factor, find out the influence law and trend of the goal changing with the factors, and seek the best combination of each factor level, this paper carries on the analysis of range and the average value of each factor at each level [15]. Through the magnitude of the range value  $R$ , it was concluded that there

was significant different effects of the factors in this experiment. The greater the range value,  $R$ , the greater the influence degree of this factor on the target, and the more critical this factor is and is the main factor. On the contrary, the smaller the range value  $R$  is, the less significant the influence degree of this factor is, and the importance of this factor is

general, which is a secondary factor. According to the test results in table 3 and figure 3, the range value  $R$ ,  $R_C > R_B > R_A$ , and the air gap spacing has the most significant and is the main factor; the influence of magnetic pole logarithm ranks second and is the second main factor; the influence of permanent magnet thickness ranks third and is a secondary factor.

Table 3. Experimental results analysis table.

| Factors value | A Thickness of permanent magnet [mm] | B Number of magnetic poles [pair] | C Air gap spacing [mm] |
|---------------|--------------------------------------|-----------------------------------|------------------------|
| K1            | 26.0                                 | 16.3                              | 53.6                   |
| K2            | 36.1                                 | 35.1                              | 30.4                   |
| K3            | 37.1                                 | 47.8                              | 15.2                   |
| k1            | 8.6                                  | 5.4                               | 17.8                   |
| k2            | 12.0                                 | 11.7                              | 10.1                   |
| k3            | 12.3                                 | 15.9                              | 5.0                    |
| R             | 3.7                                  | 10.5                              | 12.8                   |

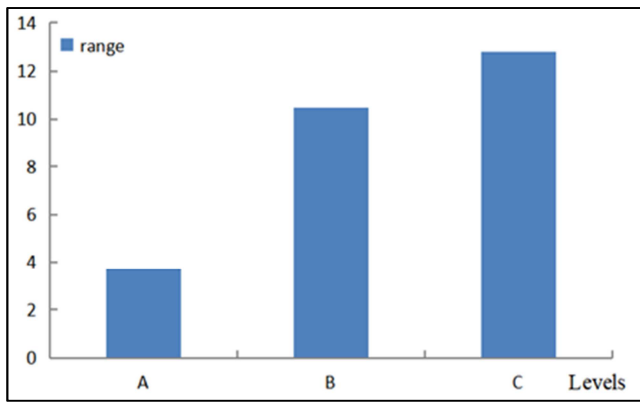


Figure 3. Primary and secondary factors of orthogonal experiment.

Table 3 shows the average values of the magnetic torque for each factor, A3, B3, and C1 are the level values with the most significant among all factors. And they are the optimal combination of factors, the permanent magnet thickness A3=10mm; the number of magnetic poles B3=12 pairs; and the air gap spacing C1=3mm. However, there is no corresponding combination scheme in the designed orthogonal test, so it is necessary to design a new scheme for numerical simulation test to verify it.

## 5. Results and Discussion

### 5.1. Numerical Simulation Test Verification

The geometric modeling of the optimized new scheme is carried out by using the three-dimensional modeling software Solidworks, The new model is imported into the finite element software Ansys Maxwell for numerical simulation. The simulation results of the original scheme and the optimized new scheme are compared and verified, the periodic curves of the output magnetic torque with time are shown in figure 4 and figure 5. The eddy current density distribution nephograms are shown in figure 6 and figure 7. The magnetic flux density distribution nephograms are shown in figure 8 and figure 9. After optimization, the

maximum magnetic torque, eddy current density distribution and magnetic flux density distribution of the new scheme is improved compared with the original scheme.

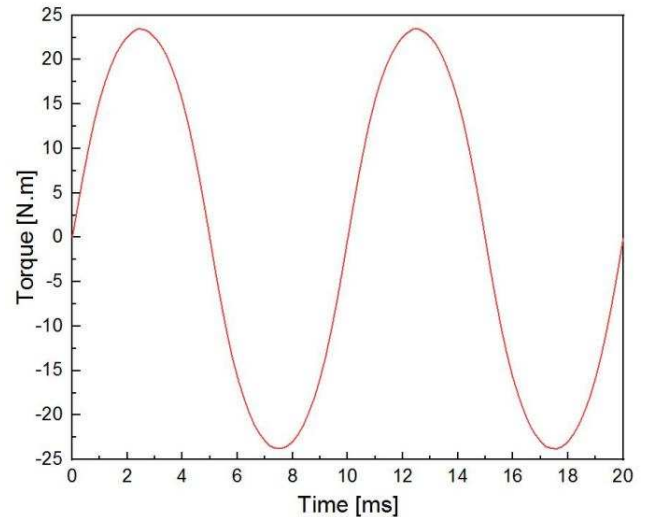


Figure 4. Magnetic torque output of the new scheme.

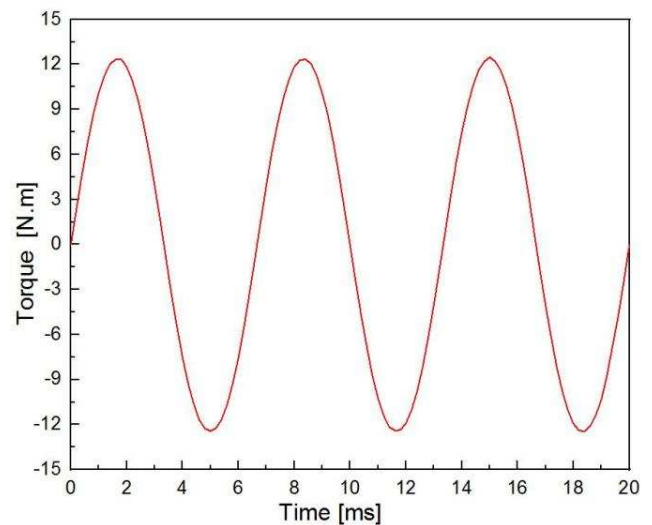


Figure 5. Magnetic torque output of the original scheme.



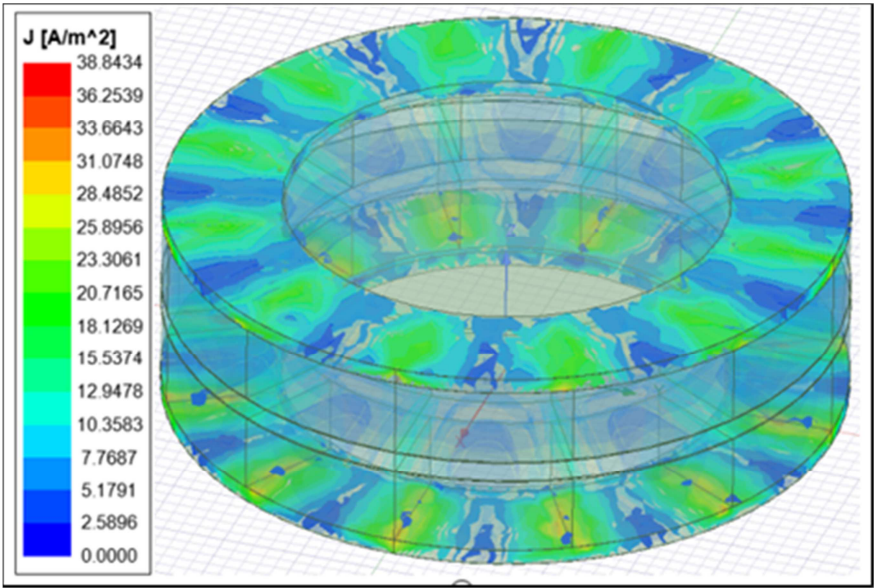


Figure 6. Eddy current density of the new scheme.

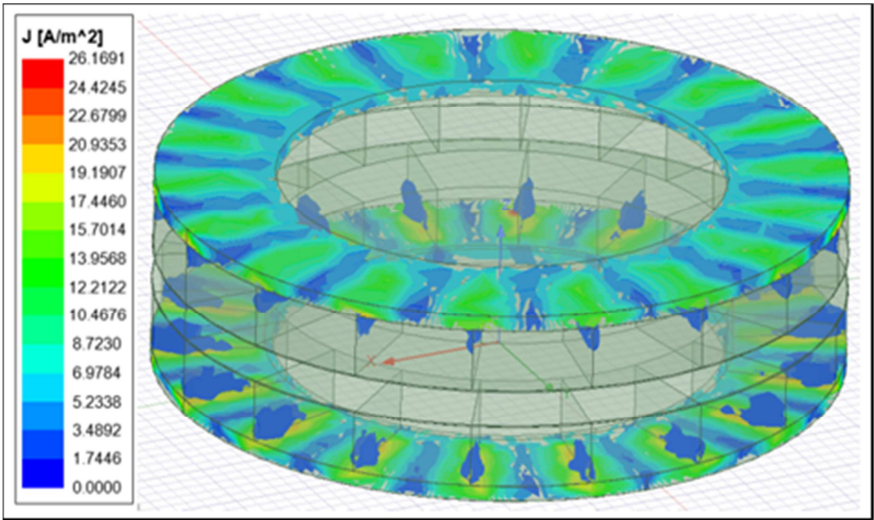


Figure 7. Eddy current density of the original scheme.

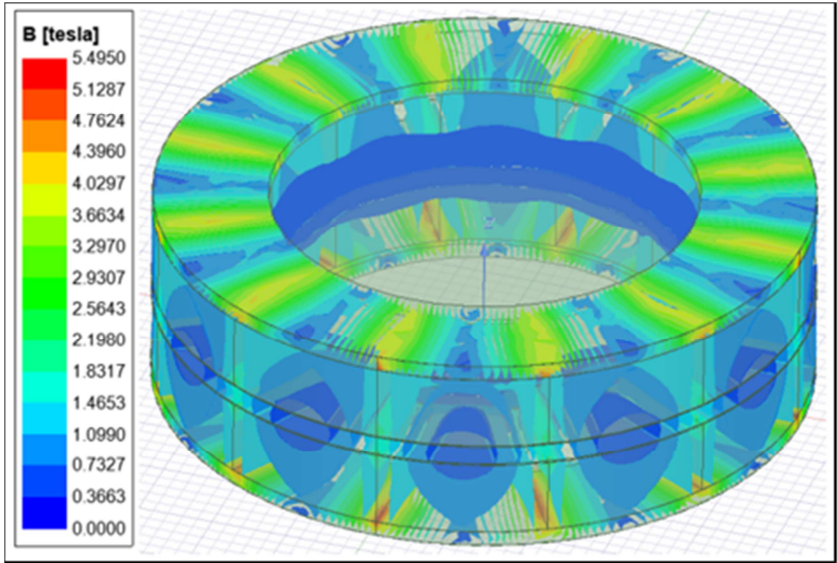


Figure 8. Magnetic flux density of the new scheme.

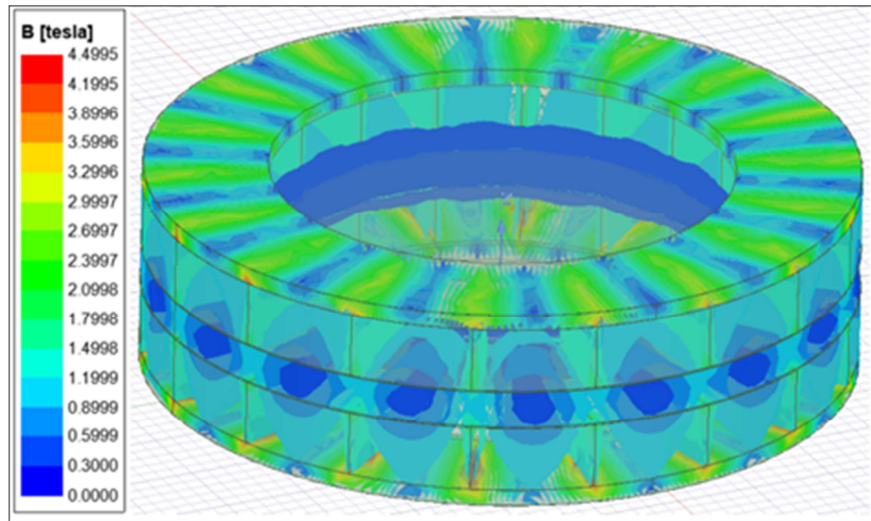


Figure 9. Magnetic flux density of the original scheme.

### 5.2. Comparison of Design Schemes Before and After Optimization

The parameters of the design scheme before and after optimization are shown in Table 4. From the simulation results of magnetic characteristics of the disk magnetic coupler before and after optimization, it can be seen that the maximum output magnetic torque  $T$  of the new scheme

after optimization is 23.5 N·m, and the maximum output magnetic torque  $T$  of the original scheme is 12.5 N·m. Compared with the original scheme, the output magnetic torque increases by 88%, which is the maximum value. After optimization, the magnetic transmission performance of the new scheme is obviously better than that of the original scheme, and the comparison of optimization results is shown in Table 5.

Table 4. Comparison of parameters before and after optimization.

| Parameter          | Permanent magnet thickness [mm] | Permanent magnet inner diameter [mm] | Permanent magnet outside diameter [mm] | Permanent magnet Width [mm] | Magnetic poles [pair] | Air gap spacing [mm] |
|--------------------|---------------------------------|--------------------------------------|--|-----------------------------|-----------------------|----------------------|
| Original design    | 8                               | 58                                   | 86                                     | 14                          | 18                    | 5                    |
| After optimization | 10                              | 58                                   | 86                                     | 14                          | 12                    | 3                    |

Table 5. Comparison of optimization results.

| Parameter          | magnetic torque [N·m] | Maximum eddy current density [ $A^2/m$ ] | Maximum magnetic flux density [T] |
|--------------------|-----------------------|--|-----------------------------------|
| Original design    | 12.5                  | 26.1                                     | 4.49                              |
| After optimization | 23.5                  | 38.8                                     | 5.49                              |
| Rate of change     | 88.0%                 | 48.6%                                    | 22.2%                             |

## 6. Summary

In this paper, a magnetic driven blender with disc magnetic coupler as the core stirring component was designed, which is to solve the problems of the traditional blender, such as short service life, easy leakage and high noise. Through finite element analysis, orthogonal experimental design, and analysis of range, the disk magnetic coupler was optimized to determine the key factors and non-key factors that affect the output magnetic torque of the disk magnetic coupler, and the level values with the most significant among all factors are A3, B3, and C1, respectively. After optimization, the optimal combination of structural parameters of the disc magnetic coupler is A3=10mm, B3=12 pairs, and C1=3mm, respectively. The experimental results show that the output magnetic torque of the optimized scheme is 23.5 N·m, which

is improved by 88% than that before optimization. Therefore, the results of this study provide a design reference for the performance optimization of disk magnetic couplers in the future.

## Conflicts of Interest

The authors declare no conflict of interest.

## Acknowledgements

This research was funded by Guangdong Provincial College Youth Innovation Talent Project (2019GKQNCX038) and Scientific Research Project of Guangdong Communication Polytechnic (GDGP-ZX-2021-001-N1).

---

## References

- [1] Yang ZiHao. (2020). Numerical Simulation and Noise Calculation of Two-phase Flow in Ultra-High Speed Flow Field of High-speed Blender [D]. School of Mechanical and Electrical Engineering, 1-92.
- [2] Qiao WeiJun. (2020). Design and Implementation of Fault Automatic Diagnosis and Protection System for Blend Machine [D]. School of Mechanical and Electrical Engineering, 1-62.
- [3] Liu Kai. (2020). Research on Testing Method of Transmission Characteristics of Magnetic Pump [D]. ZHEJIANG UNIVERSITY, 1-62.
- [4] Sun JingRu. (2018). Numerical simulation and experimental research of transmission characteristics of magnetic [D], JIANGSU UNIVERSITY, 1-95.
- [5] Du Xing. (2011). The Analysis on the Mechanical and Magnetic Performance of the High Speed Axial Magnetic Driver and the Design of the Experimental Device [D], Wuhan Textile University, 1-73.
- [6] Mo L, Zhu X, Zhang T, et al. (2018). Temperature Rise Calculation of a Flux-Switching Permanent-Magnet Double-Rotor Machine Using Electromagnetic-Thermal Coupling Analysis [J]. IEEE Transactions on Magnetics, vol. 3, 1-4.
- [7] Pan, P. Y.; Wang, D. Z.; Niu, B. W. (2021). Design optimization of APMEC using chaos multi-objective particle swarm optimization algorithm. Energy Reports, vol. 7, 531-537.
- [8] Tarvirdilu-Asl.; Rasul.; Yuksel, Murat.; Keysan, Ozan. (2019). Multi-objective design optimization of a permanent magnet axial flux eddy current brake. Turkish Journal of Electrical Engineering and Computer Sciences, vol. 27, 998-1011.
- [9] El-Wakeel, Amged, S. (2014). Design optimization of PM couplings using hybrid Particle Swarm Optimization-Simplex Method (PSO-SM) Algorithm. Electr Power Syst Res, vol. 116, 29-35.
- [10] Wang, S.; Hu, K.; Li, DY. (2019). Optimal design method for the structural parameters of hybrid magnetic coupler. Journal of Mechanical Science and Technology, vol. 33, 173-182.
- [11] Sun Feng, Ma Di, Zhao Chuan, et al. (2020). Simulation Analysis of Magnetic Characteristic of Double Permanent Magnet Wheel Linear Drive Device [J], Jixie Chuandong, vol. 3, 103-109.
- [12] YU Jiao, Shao Wan Zhen, Shi Feng, et al. (2019). Simulation Research of Disc Magnetic Coupling Based on Ansoft Maxwell [J], HYDRAULICS PNEUMATICS & SEALS, vol. 2, 32-35.
- [13] Zhao Han, Yang Zhitie, Tian Jie. (2001). Research on Calculation Method of Transmission Torque of Permanent Magnet Gear [J], Chinese Journal of Mechanical Engineering, vol. 37, 66-70.
- [14] Hua ChuXia, Wang KangJia. (2021). OPTIMIZATION OF A 3-D HIGH-POWER LED LAMP Orthogonal Experiment Method and Experimental Verification [J], THERMAL SCIENCE, vol. 25, 1495-1500.
- [15] Gong Jianlong, Zhao Yixiang, Chen Xin, et al. (2014). Multi-output Optimization on Hydrostatic Guideway Platform Based on Orthogonal Design and Comprehensive Evaluation [J], Machine Tool & Hydraulics, vol. 13, 23-26.